Internal Note: The Casimir Force in a Micron-Scale Optical Trap Geometry

Noah Kurinsky

March 24, 2015

Abstract

This

1 Background

The Casimir effect rises from zero-point energy fluctuations between conducting surfaces, which can be thought of as a result of positive feedback between stochastic deviations from the nominally non-polarized state. The nominal quantity computed in analysis of this effect is the casimir energy as a function of separation between metallic reflectors. In Casimir's classical result (Casimir, 1948) the energy between two parallel perfectly conducting plates was calculated exactly to be (Lambrecht et al., 2006)

$$\mathcal{E} = -\frac{hc\pi^2 A}{720L^3}$$

which of course makes the Casimir pressure between the two plates

$$P = \frac{1}{A}\frac{d\mathcal{E}}{dL} = \frac{hc\pi^2}{240L^4}$$

and thus in vacuum, two perfectly conducting plates at $T = 0K$ will attract each other with a pressure independent of plate area. This geometry has since been studied in various limits, including most notably finite conductivity and temperature (Lambrecht et al., 2006, and references therein) but also finite extent and non-planar geometries (Rahi et al., 2009, and references therein).

Despite the theoretical interest, the difficulty inherent in measuring the Casimir force prevented precise measurement until the landmark work of Lamoreaux (1997), who measured the force between a plate and a curved surface, to confirm the theory based on small approximations to the classical model. In this geometry, the Casimir force became an attraction with a magnitude of tens of micro dynes at separations of a few micrometers, for a plate and a small curved surface with radius of curvature of about 10cm. This work helped to solidify the theory behind finite-conductivity corrections, thermal corrections, and verify a long-used approximation called the Proximity Force Approximation (PFA, see next section) which has been used to calculate the casimir force in nearly parallel geometries.

In geometries which deviate from the non-ideal case, the calculation of the Casimir force becomes highly non-trivial. The PFA, for example, assumes that in the nearly planar limit, the Casimir force can be computed as the superposition of forces from all sets of nearly parallel subsections of the curved surface directly opposite the planar surface. It is widely known that this approximation only holds in the the limit of large curvature compared to distance, and thus for a sphere with curvature radius equal to or less than the separation between surfaces, the only analytical expression for this force is no longer strictly valid.

In the context of this experiment, this is the main barrier preventing us from producing a quick prediction for the Casimir force. Our geometry is neither spherically nor cylindrically symmetric, as the cantilever we use as a force probe has a rectangular cross-section with one

dimension much longer than the other, and the sphere is much smaller than typical separations. In addition, our cantilever is silicon coated in gold, and our bead is made of silica, whereas the normal materials dealt with are conductors thick enough that only one material correction needs to be made. Finally, we operate the bead at non-zero temperature, which requires temperature corrections which are non-trivial in the non-parallel geometry. Despite the barrier to computation of the force, it should in principle be easy to measure if we can understand the systematic effects inherent to our geometry; this is the motivation behind this note. In addition, it will most likely represent the main background we must compensate for in the measurement of other sub micron forces, namely non-newtonian gravitational corrections and chameleon models of dark energy.

In this note, I will outline the steps taken in attempting to predict the magnitude of the Casimir force we expect to measure in our experiment, beginning with the PFA, expansions to the PFA, and other simple analytical solutions. I will then cover the finite conductivity and temperature corrections, and then discuss the exact analytic and numerical solutions which exist to compensate for these non-idealities. I will present predictions, and discuss other approaches we have attempted and potential limitations of the calculations. The idea will be that it is left up to those more theoretically inclined to compute the exact theoretical prediction to our model, but that we should be able to come up with a prediction to within 10-20% of the true Casimir force as a function of distance. I will conclude by discussing the reason for the limitations and assumptions.

2 Analytical Spherical Solutions

The only exact solutions come for the

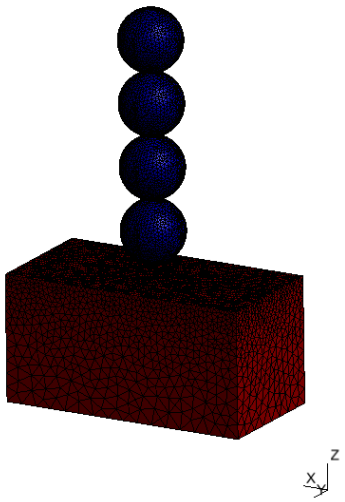

Figure 1: Geometry of cantilever and bead, truncated in the x direction and limited to tens of plasma wavelengths in depth. Here we show four distances of the bead from the cantilever in the z direction.

2.1 Proximity Force Approximation (PFA)

2.2 Expanded Proximity Force Approximation

Most of this section taken from Fosco et al. (2011), also see Bimonte et al. (2012)

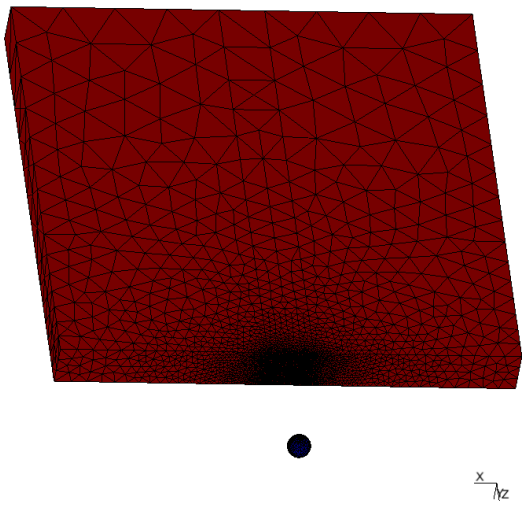

Figure 2: Geometry of cantilever and bead, representing the full x-y shape of the cantilever and extended to 100 plasma wavelengths in depth. Here we show the bead 20 microns from the cantilever in the z direction.

Normal energy of Casimir Effect:

$$E_{pp}(z) = -\frac{\pi^2}{1440 z^3}$$

For $R >> a$:

$$E_C \approx E_{PFA} = \int_\Sigma E_{pp}(z) d\sigma$$

We don't expect this to hold much past this condition, but can use the derivative expansion to first order to obtain a slightly more accurate term. The formula for the derivative expansion in terms of some surface separation $z = \psi(\mathbf{x}_\parallel)$ is

$$E_{DE} = -\frac{\pi^2}{1440} \int \frac{1}{\psi^3} \left(1 + \frac{2}{3}(\partial_\alpha \psi)^2\right) d\mathbf{x}_\parallel$$

and if we add in the correction factor $\eta_E(z)$ (see next section), we get

$$E_{DE} = -\frac{\pi^2}{1440} \int \frac{\eta_E(\psi)}{\psi^3} \left(1 + \frac{2}{3}(\partial_\alpha \psi)^2\right) d\mathbf{x}_\parallel$$

which, given the complexity of η_E, is best evaluated numerically. We can parameterize the surface of a sphere as

$$\psi_0(r) = R\left(1 - \sqrt{1 - \frac{r^2}{R^2}}\right)$$

where the surface separation would be $\psi = a + \psi_0(r)$ and a the minimal separation between sphere and plane. Given that the derivative with respect to θ is 0, the integral simplifies to

$$E_{DE} = -\frac{2\pi^3}{1440} \int \frac{\eta_E(\psi)}{\psi^3} \left(1 + \frac{2}{3}(\partial_r \psi)^2\right) dr$$

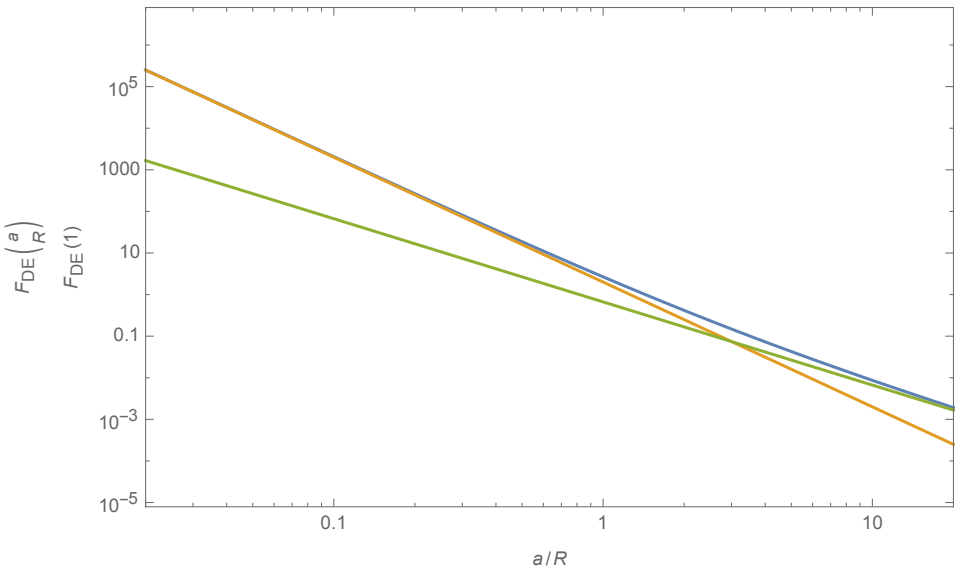

Figure 3: Illustration of the effect of the first order correction on the PFA; blue line shows expansion, orange line is PFA, green line is first order correction.

and we can write, as well,

$$(\partial_r \psi)^2 = R^2 \left[-\frac{1}{2} \left(1 - \frac{r^2}{R^2} \right)^{-1/2} \left(\frac{-2r}{R^2} \right) \right]^2 = \frac{r^2}{R^2(1 - \frac{r^2}{R^2})} = \frac{r^2}{R^2 - r^2} = \left(\frac{R^2}{r^2} - 1 \right)^{-1}$$

we can see that the derivative is undefined if we integrate to R, so as long as we integrate to $r_{limit} < R$ we should have a convergent integral; this shouldn't affect the accuracy given the r^{-3} dependence. The effect of the derivative expansion correction in a perfectly conducting system can be seen below.

Bulgac et al. (2006) calculate the force between plane and sphere exactly, and compare to PFA. Canaguier-Durand et al. (2012) explore various temperature and geometry effects as a function of radius and separation.

3 Finite Conductivity Corrections

3.1 Dielectric Correction

Bimonte et al. (2012); Lambrecht and Reynaud (2000): dielectric effects, non-perfect conductivity. The following mostly from Lambrecht and Reynaud (2000)

The dielectric constant is large at frequencies smaller than the plasma frequency ω_p, so corrections are more relevant at separations smaller than the plasma wavelength

$$\lambda_p = \frac{2\pi c}{\omega_p}$$

where

$$\omega_p^2 = \frac{Nq^2}{\epsilon_0 m^*} = \frac{ZN_a q^2}{\epsilon_0 m^*} = \frac{\rho q^2}{\epsilon_0 m^* m_z}$$

and in turn, N is the number of conduction electrons per unit volume, Z is the number of free electrons per atom (taken to just be $Z = 1$), N_a is the atomic number density, q is the electron charge, and m^* is effective electron mass, also taken to be 1 for Au though not necessarily for SiO^2. We in turn calculate N_a as the density ρ divided by the atomic mass m_Z for the species.

Thermal corrections relevant at distances larger than

$$\lambda_T = \frac{\hbar c}{k_B T}$$

The reduction factor for the Casimir energy is given by

$$\eta_E = -\frac{180L^3}{c\pi^4}\int_0^\infty \kappa d\kappa \int_0^{c\kappa} \sum_{p=\parallel,\perp} \log\left(1 - r_{p,1}(i\omega, i\kappa) r_{p,2}(i\omega, i\kappa) e^{-2\kappa L}\right) d\omega \tag{1}$$

where $r_{p,i}(i\omega, i\kappa)$ is the reflection amplitude of surface i for polarization p, where $i\omega$ is the imaginary frequency and $i\kappa$ is the imaginary wave vector along the longitudinal direction of the cavity, or the normal to the plane. The reflection coefficients for thick slabs are given by

$$r_\perp = -\frac{\sqrt{\omega^2(\epsilon(i\omega) - 1) + c^2\kappa} - c\kappa}{\sqrt{\omega^2(\epsilon(i\omega) - 1) + c^2\kappa} + c\kappa} \tag{2}$$

$$r_\parallel = \frac{\sqrt{\omega^2(\epsilon(i\omega) - 1) + c^2\kappa} - c\kappa\epsilon(i\omega)}{\sqrt{\omega^2(\epsilon(i\omega) - 1) + c^2\kappa} + c\kappa\epsilon(i\omega)} \tag{3}$$

Lambrecht and Reynaud (2000) suggest numerical integration over the range 10^{-4} to 10^3 eV for distances 0.1 to 10 μm

3.2 Expected accuracy

We are limited by the validity of the proximity force approximation, which assumes the (roughly) Casimir forces are additive, which is known not to be the case, and assumes the sphere and plane are close enough such that the plane appears infinite and the curvature is relatively small. We include the first order correction to the PFA, which may not extend validity very far and still assumes the plane is long enough to be effectively infinite.

4 Numerical Computation

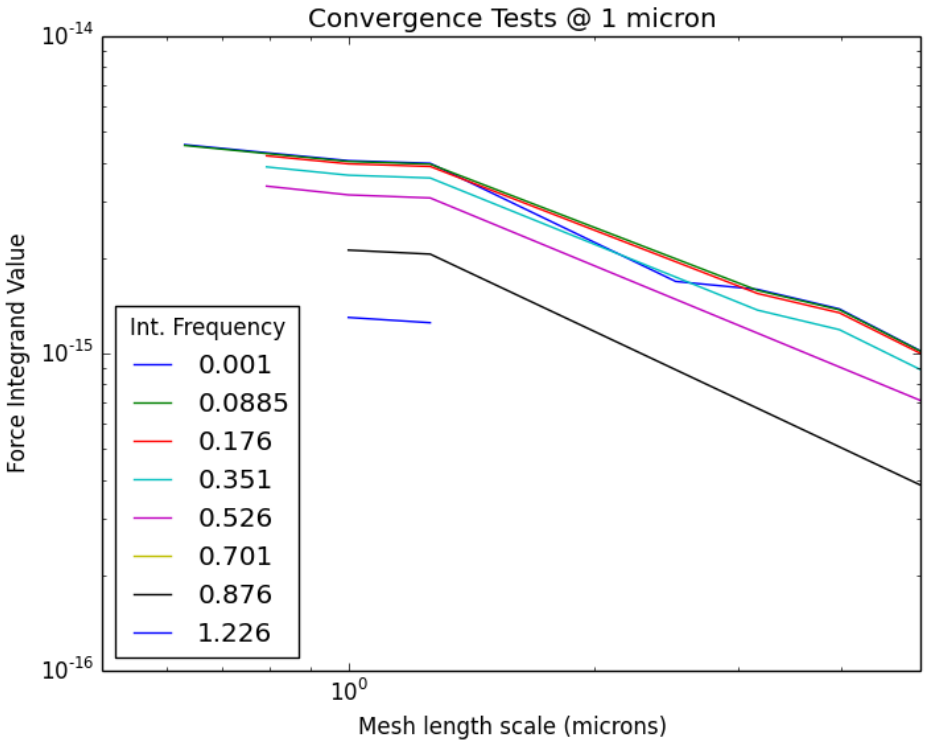

Figure 4: Earlier Casimir force estimates based on different geometries.

A Scuff-EM

B Casimir Force Code

References

G. Bimonte, T. Emig, R. L. Jaffe, and M. Kardar. Casimir forces beyond the proximity approximation. *EPL (Europhysics Letters)*, 97:50001, March 2012. doi: 10.1209/0295-5075/97/50001.

Giuseppe Bimonte, Thorsten Emig, and Mehran Kardar. Material dependence of casimir forces: Gradient expansion beyond proximity. *Applied Physics Letters*, 100(7):074110, 2012. doi: http://dx.doi.org/10.1063/1.3686903. URL `http://scitation.aip.org/content/aip/journal/apl/100/7/10.1063/1.3686903`.

Aurel Bulgac, Piotr Magierski, and Andreas Wirzba. Scalar casimir effect between dirichlet spheres or a plate and a sphere. *Phys. Rev. D*, 73:025007, Jan 2006. doi: 10.1103/PhysRevD.73.025007. URL `http://link.aps.org/doi/10.1103/PhysRevD.73.025007`.

Antoine Canaguier-Durand, Romain Guerot, Paulo A. Maia Neto, Astrid Lambrecht, and Serge Reynaud. The casimir effect in the sphere-plane geometry. *International Journal of Modern Physics: Conference Series*, 14:250–259, 2012. doi: 10.1142/S2010194512007374. URL `http://www.worldscientific.com/doi/abs/10.1142/S2010194512007374`.

H.B.G. Casimir. On the Attraction Between Two Perfectly Conducting Plates. *Indag.Math.*, 10:261–263, 1948.

D (μm)	F (aN)	D (μm)	F (aN)
3	7.37e+01	16	2.34e-01
4	2.90e+01	17	1.85e-01
5	1.38e+01	18	1.47e-01
6	7.61e+00	19	1.19e-01
7	4.61e+00	20	9.71e-02
8	2.96e+00	21	7.99e-02
9	1.97e+00	22	6.63e-02
10	1.35e+00	23	5.54e-02
11	9.53e-01	24	4.66e-02
12	6.92e-01	25	3.95e-02
13	5.14e-01	26	3.36e-02
14	3.89e-01	27	2.87e-02
15	3.00e-01	28	2.47e-02
		29	2.13e-02

Table 1: Force as function of distance, silica bead and gold cantilever, in microns and attonewtons respectively. This points interpolated between slightly sparser points (5,10,15,20,25,30 are exact calculations) and have relative uncertainty on the 10% level to high confidence.

César D. Fosco, Fernando C. Lombardo, and Francisco D. Mazzitelli. Proximity force approximation for the casimir energy as a derivative expansion. *Phys. Rev. D*, 84:105031, Nov 2011. doi: 10.1103/PhysRevD.84.105031. URL `http://link.aps.org/doi/10.1103/PhysRevD.84.105031`.

A. Lambrecht and S. Reynaud. Casimir force between metallic mirrors. *European Physical Journal D*, 8:309–318, July 2000. doi: 10.1007/s100530050041.

A. Lambrecht, P. A. M. Neto, and S. Reynaud. The Casimir effect within scattering theory. *New Journal of Physics*, 8:243, October 2006. doi: 10.1088/1367-2630/8/10/243.

S. K. Lamoreaux. Demonstration of the casimir force in the 0.6 to 6μ m range. *Phys. Rev. Lett.*, 78:5–8, Jan 1997. doi: 10.1103/PhysRevLett.78.5. URL `http://link.aps.org/doi/10.1103/PhysRevLett.78.5`.

Sahand Jamal Rahi, Thorsten Emig, Noah Graham, Robert L. Jaffe, and Mehran Kardar. Scattering theory approach to electrodynamic casimir forces. *Physical Review D*, 80(8), 2009. doi: 10.1103/PhysRevD.80.085021.

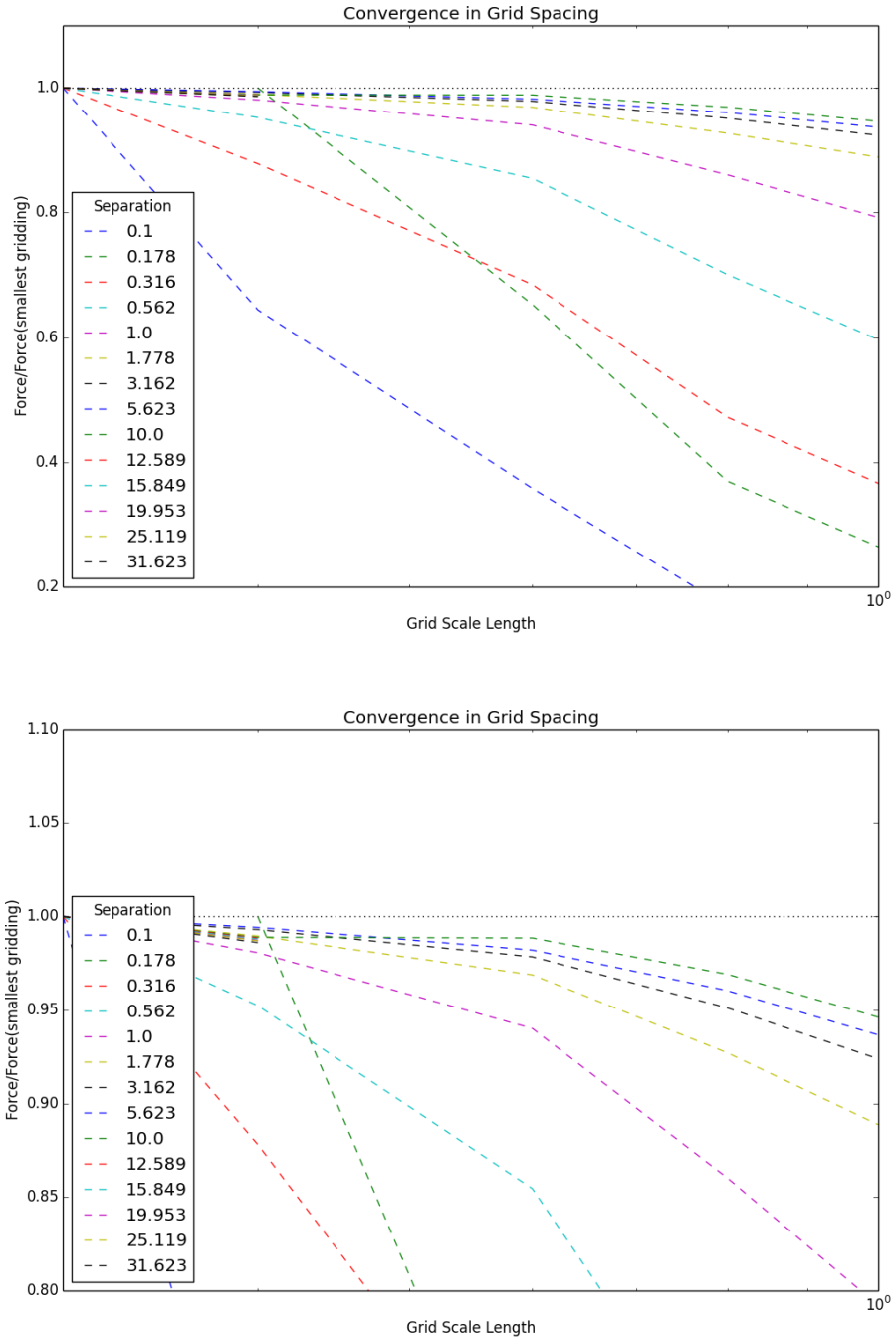

Figure 5: Earlier Casimir force estimates based on different geometries.

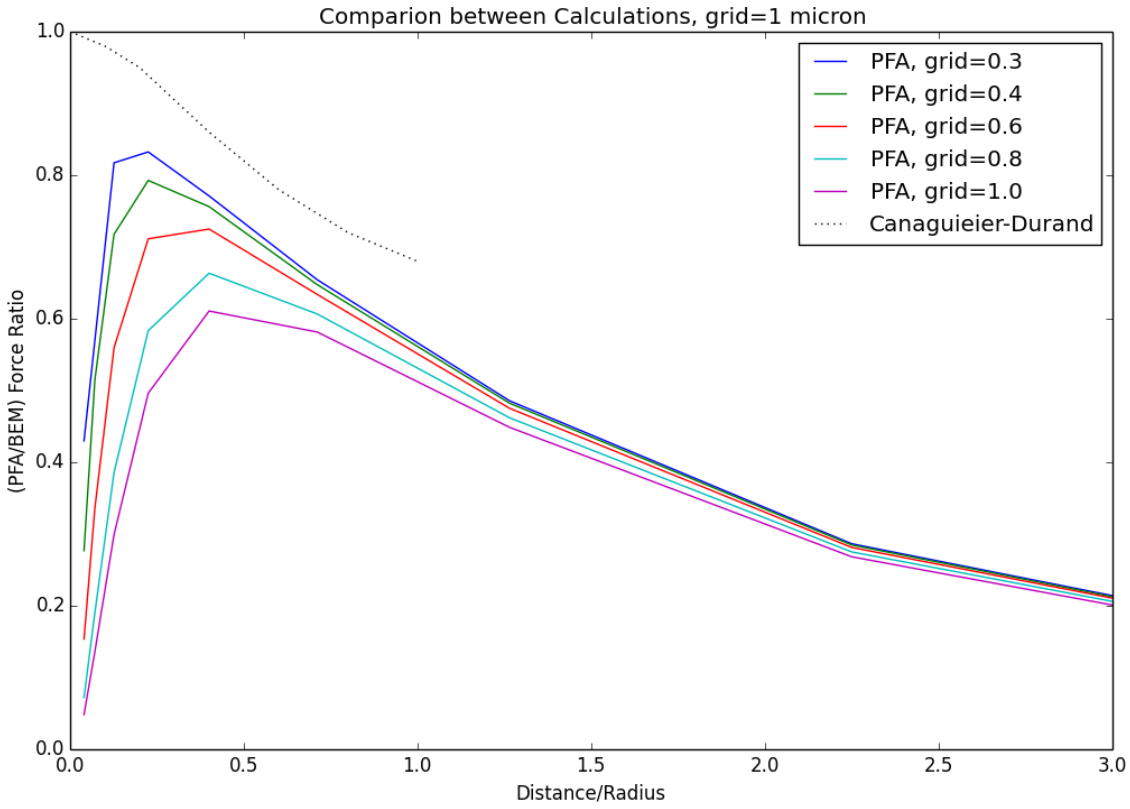

Figure 6: Earlier Casimir force estimates based on different geometries.

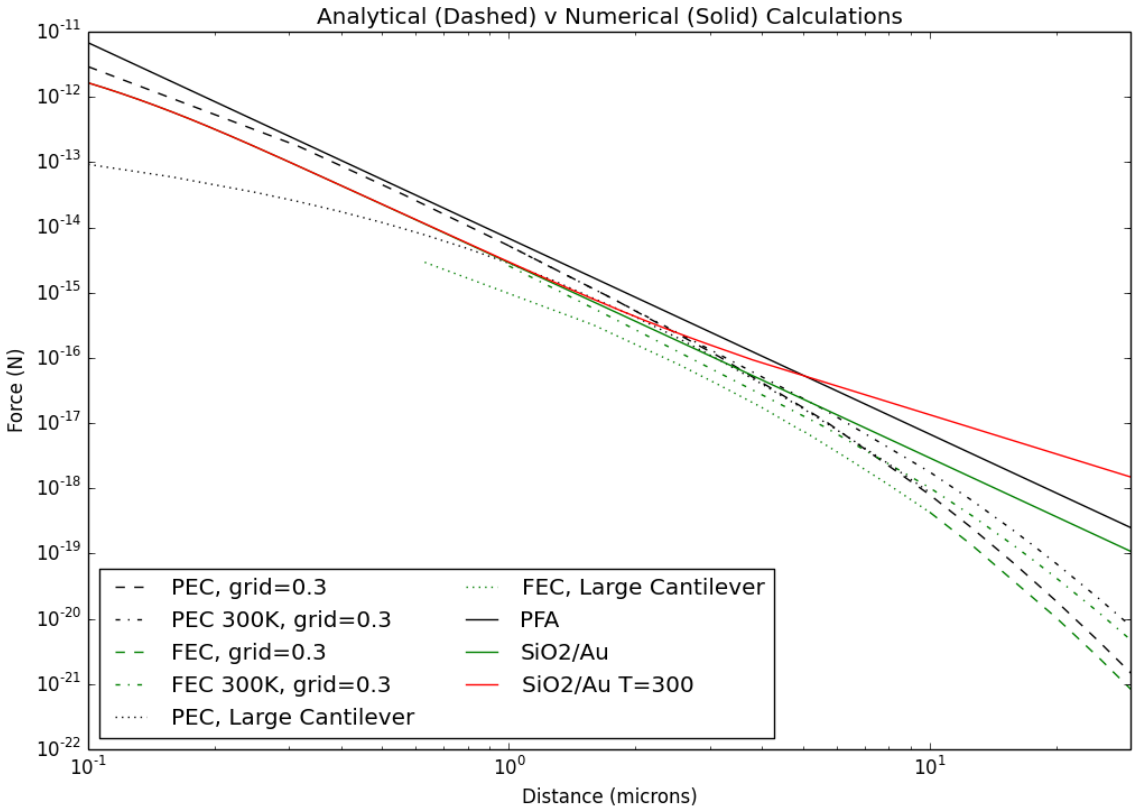

Figure 7: Earlier Casimir force estimates based on different geometries.

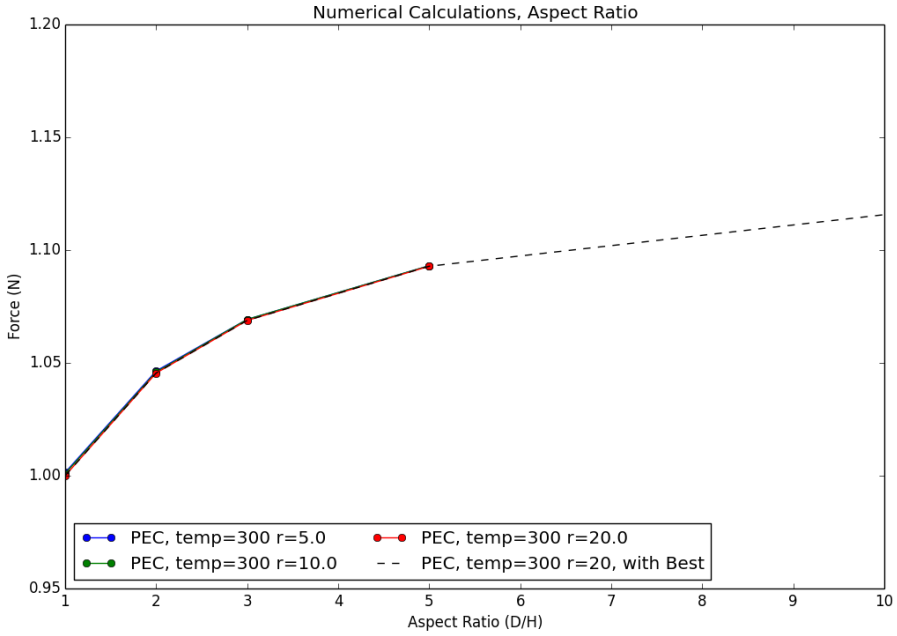

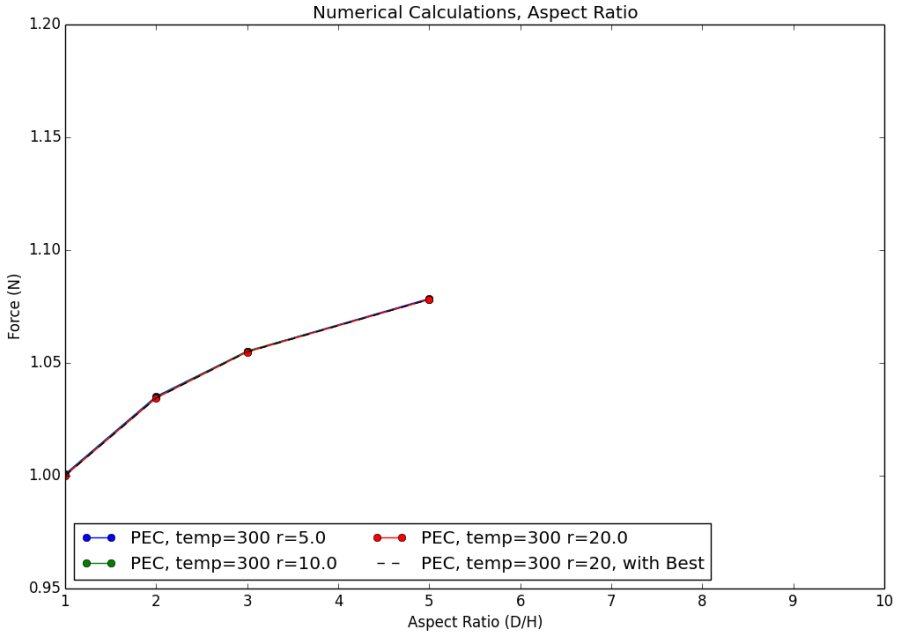

Figure 8: Depth versus relative grid size on the rear of the cantilever, showing relatively little dependence on relative grid size but large dependence on overall depth (fine grinding not as important as there being cells).

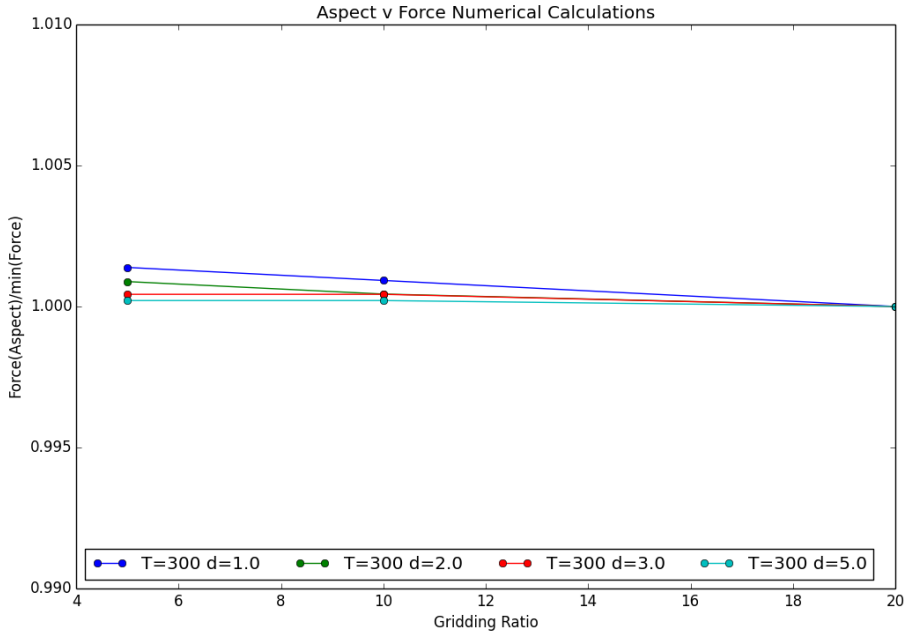

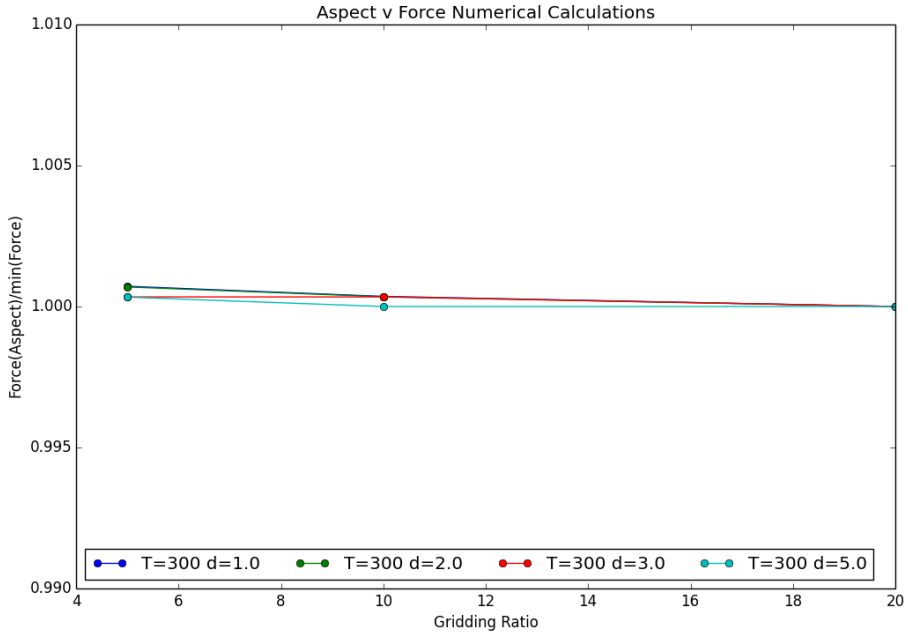

Figure 9: Depth versus relative grid size on the rear of the cantilever, showing relatively little dependence on relative grid size but large dependence on overall depth (fine grinding not as important as there being cells).

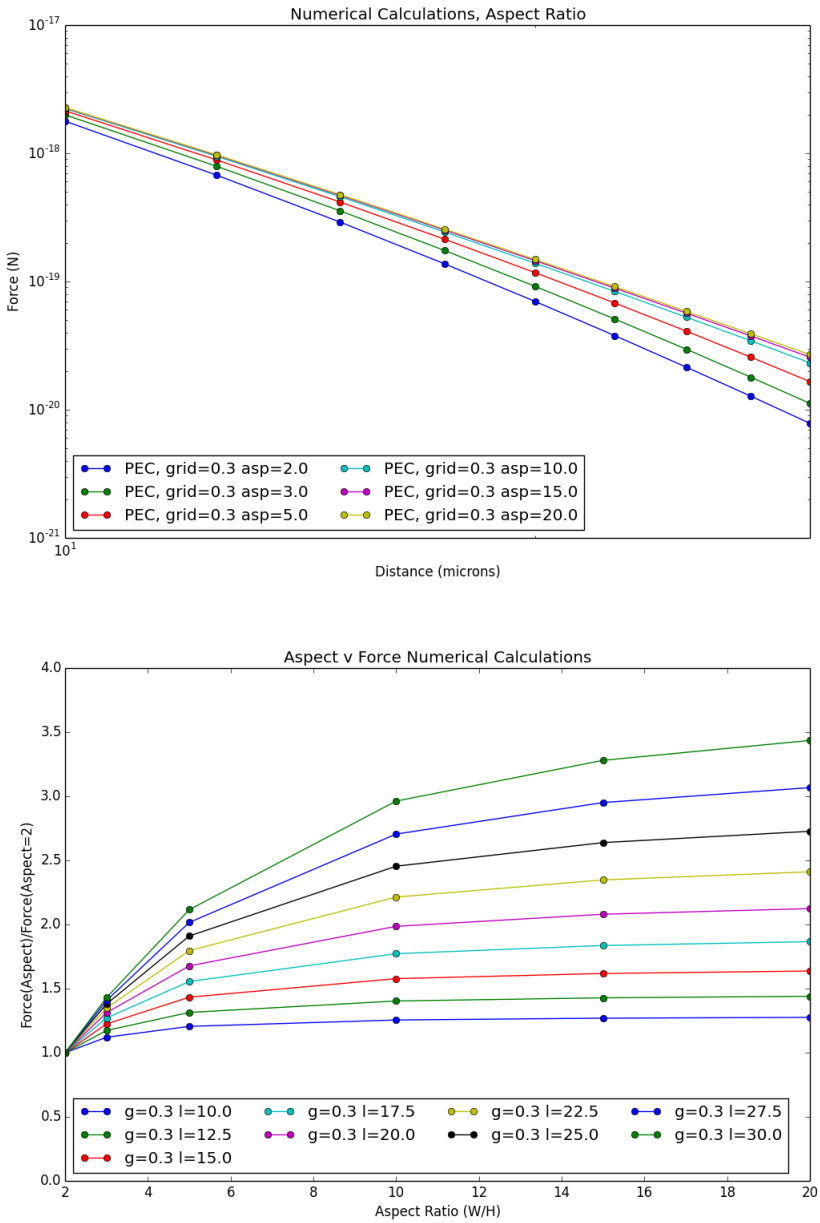

Figure 10: Width (in terms of aspect ratio) versus distance from the cantilever, showing increased variation of value from that at aspect ratio of 2 as separation increases (which makes sense geomertically). The cantilever we utilize corresponds to an aspect ratio of 10.

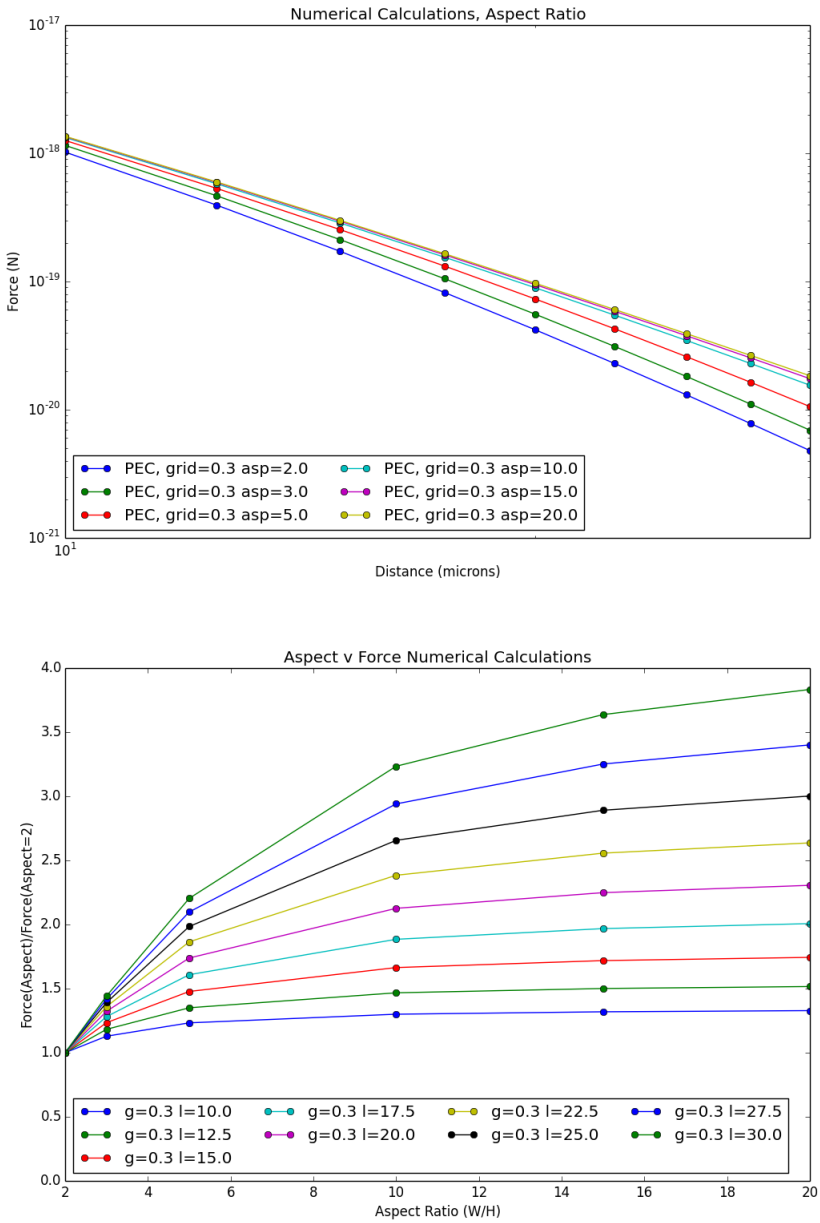

Figure 11: Width (in terms of aspect ratio) versus distance from the cantilever for finite conductivity, showing increased variation of value from that at aspect ratio of 2 as separation increases (which makes sense geomertically). The cantilever we utilize corresponds to an aspect ratio of 10.

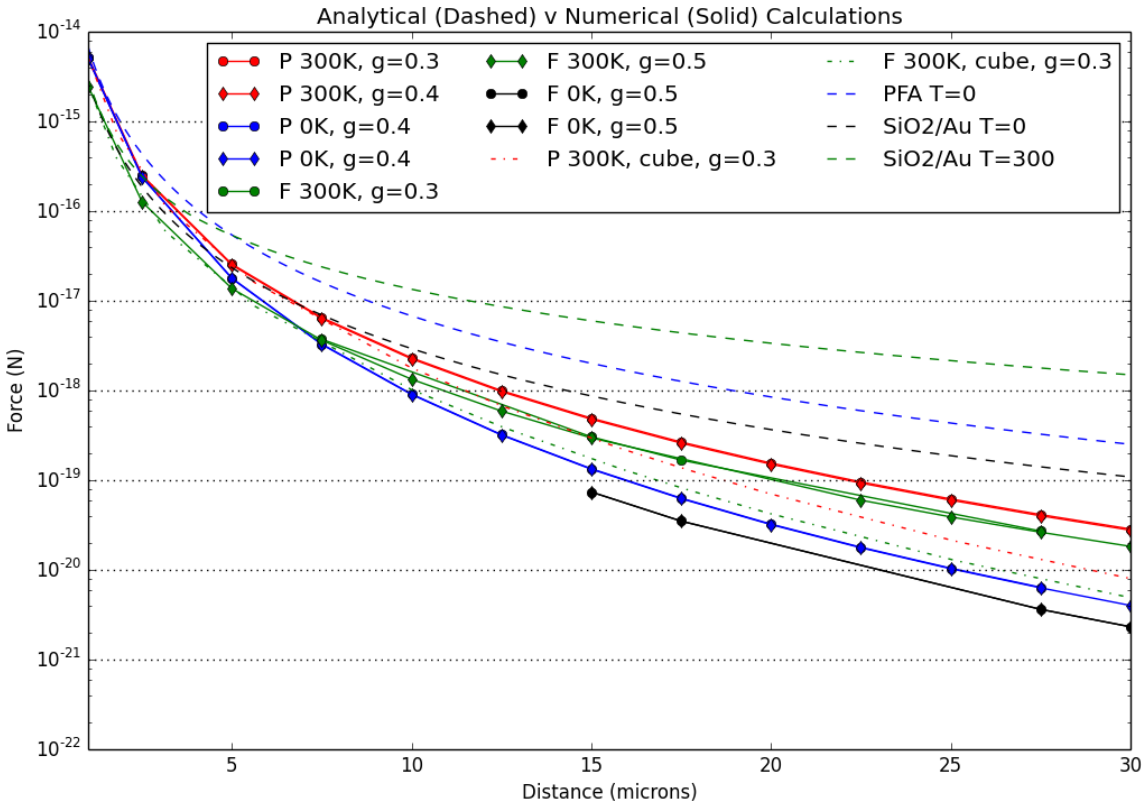

Figure 12: Casimir force estimate based on extended geometry.

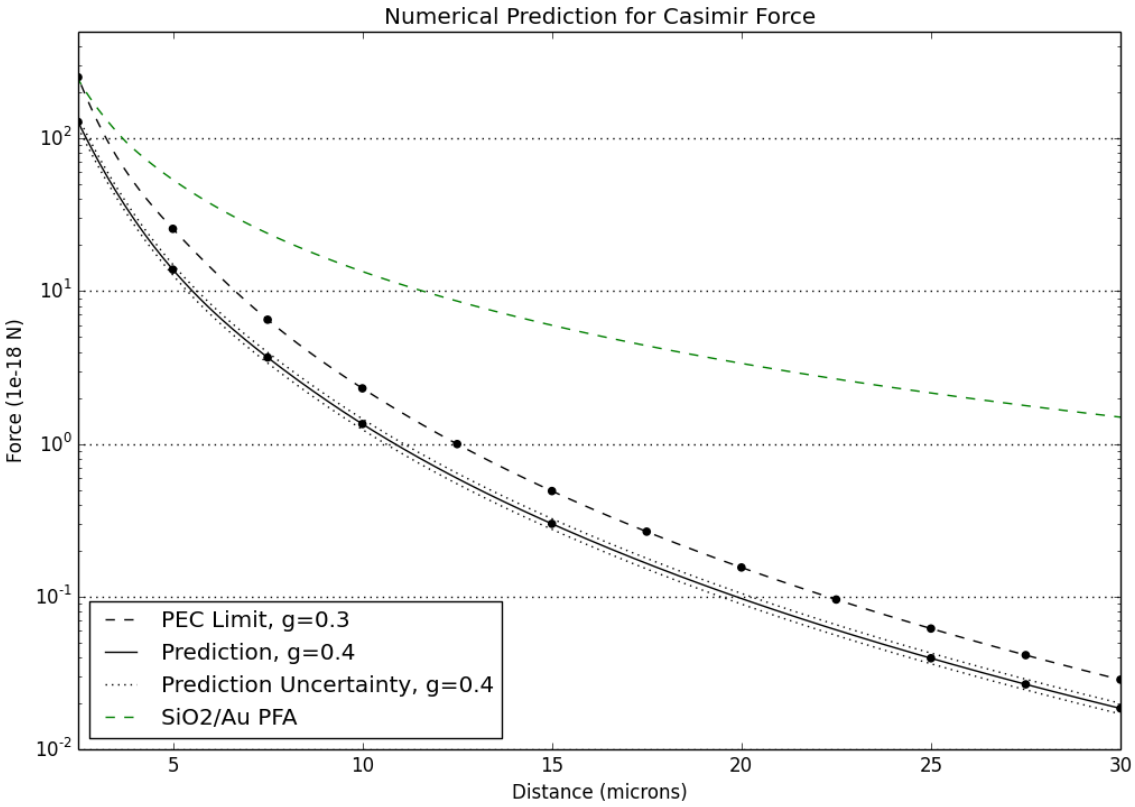

Figure 13: Best prediction for Casimir force at 300K with finite conductivity correction.

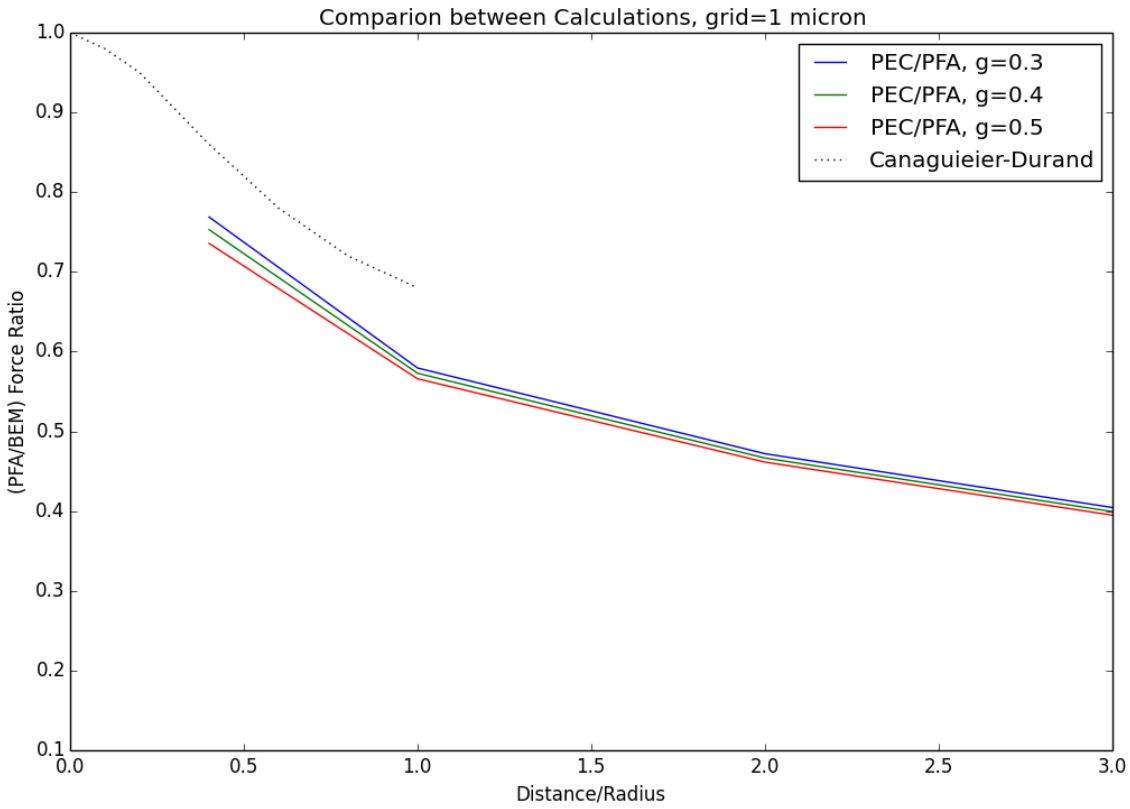

Figure 14: Casimir force estimates compared to PFA, based on large geometry. Compared to correction for infinite plane.

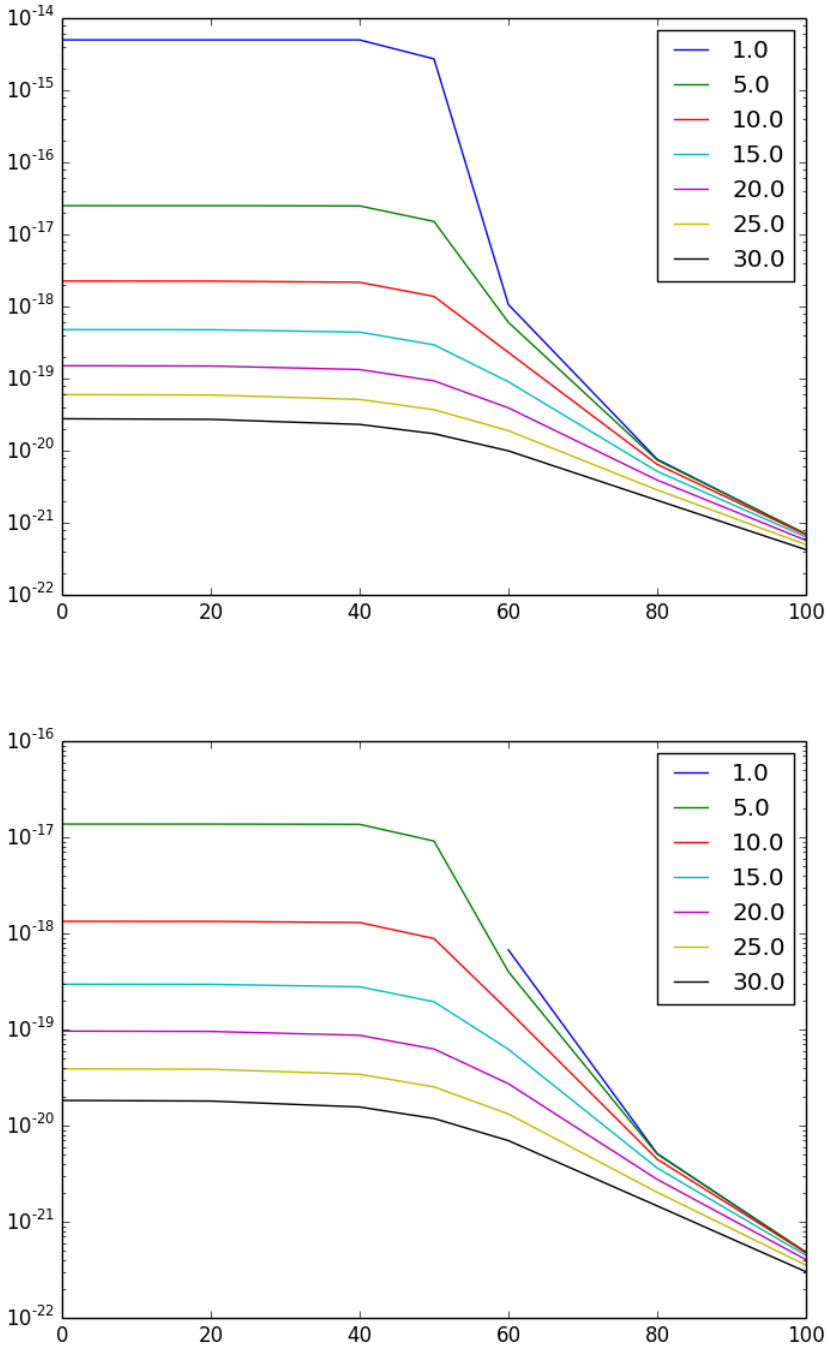

Figure 15: Force as a function of lateral displacement along the cantilever.

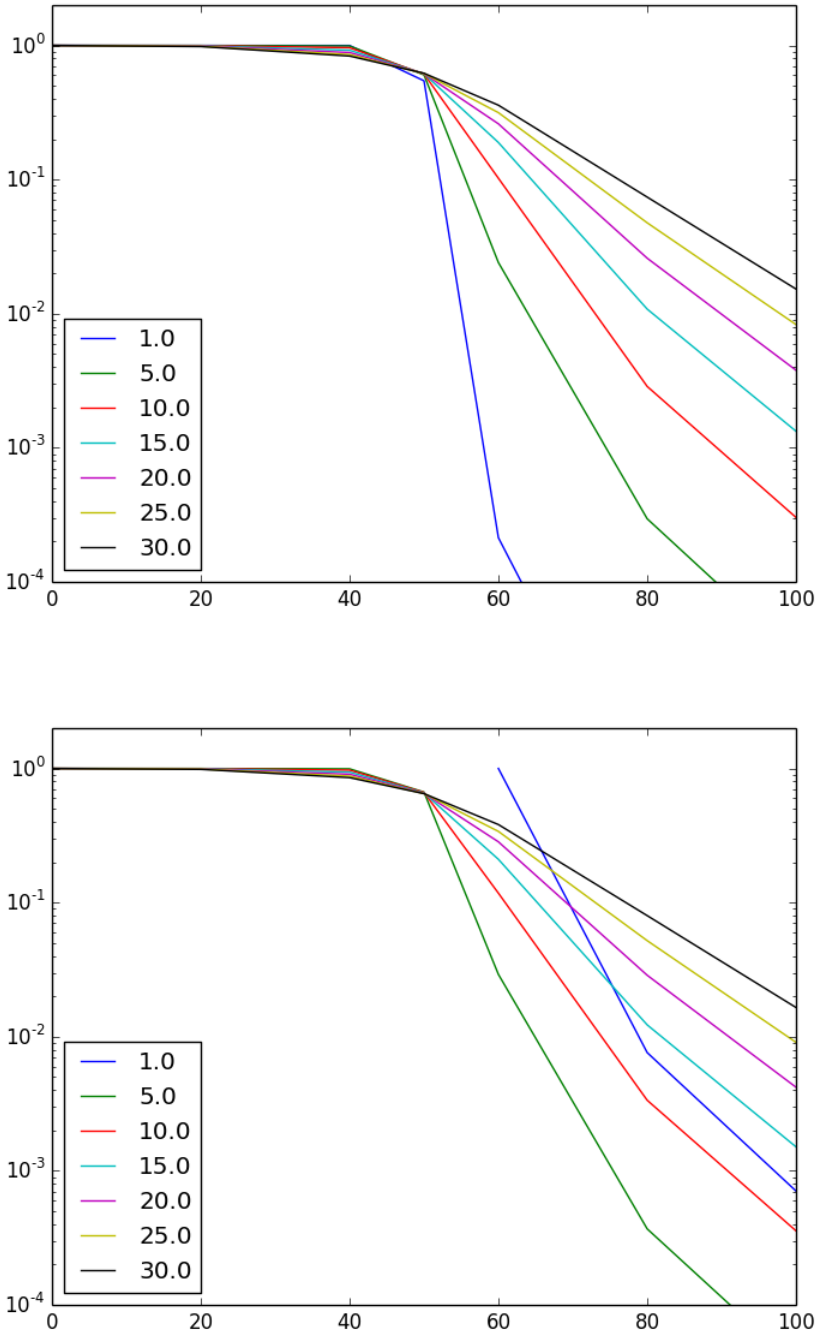

Figure 16: Force ratio as a function of lateral displacement along the cantilever.

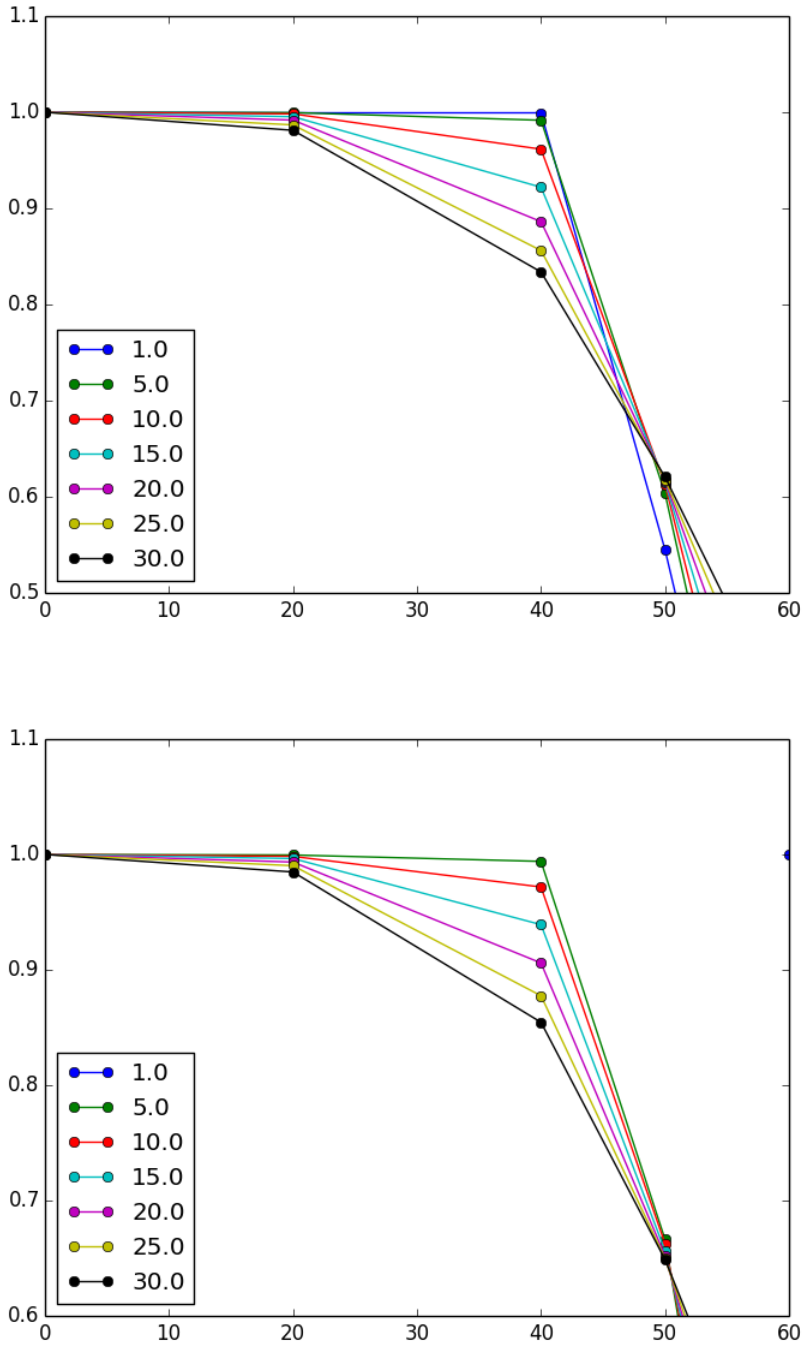

Figure 17: Force ratio as a function of lateral displacement along the cantilever.